Carbohydrate Polymers 106 (2014) 60–70

Contents lists available at ScienceDirect

Carbohydrate Polymers

journal homepage: www.elsevier.com/locate/carbpol

Thermal degradation behavior and kinetic analysis of spruce glucomannan and its methylated derivatives

Rosana Moriana[a], Yujia Zhang[a], Petra Mischnick[b], Jiebing Li[a,c], Monica Ek[a,*]

[a] Department of Fibre and Polymer Technology, Royal Institute of Technology-KTH, SE-100 44 Stockholm, Sweden
[b] Department of Food Chemistry, Technische Universität Braunschweig, Schleinitzstraße 20, D-38106 Braunschweig, Germany
[c] Wallenberg Wood Science Center, The Royal Institute of Technology and Chalmers University of Technology, SE-100 44 Stockholm, Sweden

ARTICLE INFO

Article history:
Received 13 December 2013
Received in revised form 22 January 2014
Accepted 25 January 2014
Available online 2 February 2014

Keywords:
Spruce glucomannan
Konjac glucomannan
Methylated glucomannan
Thermogravimetry
Thermal degradation behavior
Kinetic triplet

ABSTRACT

The thermal degradation behavior and kinetics of spruce glucomannan (SGM) and its methylated derivatives were investigated using thermogravimetric analysis to characterize its temperature-dependent changes for use in specific applications. The results were compared with those obtained for commercial konjac glucomannan (KGM). The SGM and the KGM exhibited two overlapping peaks from 200 to 375 °C, which correspond to the intensive devolatilization of more than 59% of the total weight. Differences in the pyrolysis-product distributions and thermal stabilities appeared as a result of the different chemical compositions and molecular weights of the two GMs. The Friedman and Flynn-Wall-Ozawa isoconversional methods and the Coats–Redfern were adopted to determine the kinetic triplet of the intensive devolatilization region. Both GMs can be modeled using a complex mechanism that involves both a Dn-type and an Fn-type reaction. The comparative study of partially methylated GM indicated higher homogeneity and thermal resistance for the material with the higher degree of substitution.

1. Introduction

Hemicelluloses are structural carbohydrates of plant cell walls that, in close association with cellulose and lignin, form the lignocellulosic biomass. Hemicelluloses generally occur as heteropolysaccharides, in which their main building units are hexoses (D-glucose, D-mannose and D-galactose) and pentoses (D-xylose and L-arabinose). Small amounts of deoxyhexoses (L-rhamnose and L-fucose) and uronic acids (4-*O*-methyl-D-glucuronic acid, D-galacturonic acid and D-glucuronic acid) are also present. Hemicelluloses have a lower degree of polymerization (DP) and are more easily hydrolyzed and less thermally stable than cellulose. An understanding of their pyrolytic behavior is of paramount importance in improving process fundamentals and designing effective biomass-conversion technologies, such as the torrefaction process, which is carried out at the typical degradation temperature of hemicelluloses (Branca, Di Blasi, Mango, & Hrablay, 2013; Chaouch, Pétrissans, Pétrissans, & Gérardin, 2010). In general, in thermochemical conversion technologies, pyrolysis plays a key role in determining the reaction kinetics, and it is therefore critical to reactor design and the determination of product distribution, composition and properties (Raveendran, Ganesh, & Khilar, 1995). Pyrolysis studies are also essential to implementing new biomass-conversion technologies, such as low-temperature carbonization and chemical production from solid fuels (Seo, Park, Hwang, & Yu, 2010). A significant number of studies are available concerning the pyrolysis of xylan from hardwood hemicelluloses (Bilbao, Millera, & Arauzo, 1989; Di Blasi & Lanzetta, 1997; Shen, Gu, & Bridgwater, 2010). In contrast, no study is available regarding the thermal behavior, thermal degradation kinetics and products of pyrolysis of softwood glucomannan, which is the main component of softwood hemicellulose.

The thermal and kinetic aspects of solid state decomposition reactions are complex (Yang, Miranda, & Roy, 2001) and involve a large number of parameters to investigate. Thermogravimetric analysis (TGA) is one of the most widely used techniques to assess the thermal and kinetic behavior of carbohydrate polymers, allowing the determination of parameters such as the kinetic triplet, which includes (Nelson David, Hallen Richard, & Theander, 1988) the apparent activation energy, the reaction mechanism ($f(\alpha)$) and the pre-exponential factor (A) (Akbar, Iqbal, Massey, & Masih, 2012; Iqbal, Massey, Akbar, Ashraf, & Masih, 2013; Moriana, Vilaplana, Karlsson, & Ribes-Greus, 2011; Yao, Wu, Lei, Guo, & Xu, 2008;

* Corresponding author at: Division of Wood Chemistry and Pulp Technology, School of Chemical Science and Engineering, KTH Royal Institute of Technology, Teknikringen 56, SE 10044 Stockholm, Sweden. Tel.: +46 08 790 81 04; fax: +46 08 790 6166.
E-mail address: monicaek@kth.se (M. Ek).

0144-8617/$ – see front matter © 2014 Elsevier Ltd. All rights reserved.
http://dx.doi.org/10.1016/j.carbpol.2014.01.086

Zohuriaan & Shokrolahi, 2004); the thermal stability and the distribution of pyrolysis products (Ramajo-Escalera, Espina, García, Sosa-Arnao, & Nebra, 2006; Wilson, Yang, Blasiak, John, & Mhilu, 2011); and the proximate analysis data, including the calorific value (García, Pizarro, Lavín, & Bueno, 2013).

There are other technologies related to thermal processing that also require the superior materials characterization offered by TGA to predict their temperature dependence and to solve the drawbacks related to their temperature sensitivity. Biomass can be processed by extrusion, injection and compression molding to design sustainable materials as an alternative to synthetic polymers. To do this, knowledge of the thermal degradation kinetics and behavior is of practical relevance for understanding and predicting the thermal resistance and degradation of materials to be used for specific applications (Aggarwal, Dollimore, & Heon, 1997). Among all the hemicellulose components, hexoses are known to be less susceptible to hydrolysis and dehydration reactions than pentoses (Akbar et al., 2012). Therefore, glucomannan is thermally more stable than xylan (C. Ramos-Sanchez, Rey, L. Rodriguez, Martin-Gil, & Martin-Gil, 1988). This property, together with other properties, such as its viscosity (Xue Jiao He, Amadou, & Qin, 2012) and renewability (Kohyama, Kim, Shibuya, Nishinari, & Tsutsumi, 1992), render glucomannan carbohydrates as one of the most interesting hemicellulose polymers to be applied in materials science. In this sense, several approaches have been reported in the literature with interesting results. Cheng, Abd Karim, and Seow (2008) made emulsion films from carboxymethyl cellulose and deacetylated konjac glucomannan (KGM) with a higher barrier and mechanical efficiency. Mikkonen et al. (2010) studied the thermal properties of films based on KGM and spruce galactoglucomannans with cellulose nanowhiskers. Enomoto-Rogers, Ohmomo, and Iwata (2013) used KGM as a thermoplastic and evaluated differences in its thermal stability as a function of the degree of acetylation (DS_{Ac}), showing an improvement with increasing DS_{Ac} of the KGM.

In this study, spruce glucomannan (SGM) was selected for thermal assessment from among the other potential hemicellulose polymers because no detailed study has previously been conducted to determine its thermal degradation behavior and kinetics. The scope of this work includes the development of an appropriate methodology for gathering suitable information regarding the pyrolysis-product distribution, heating value, thermal stability and kinetic triplet of a glucomannan polymer. These parameters are useful in understanding and predicting the thermal behavior of glucomannan to define its potential for use in bioenergy or as a material that is resistant enough to be processed using conventional thermal technologies and/or to have a competitive service life. SGM was extracted from softwood and was later modified *via* methylation to obtain various degree of substitution (DS). The influence of the DS value on the thermal behavior was also explored, and all results were compared with those of a well-established commercial KGM (Kohyama et al., 1992).

2. Experimental

2.1. Materials

Spruce (Picea abies) wood chips were obtained from the Södra Cell Värö mill in Sweden. The wood chips were cut into 1 cm wide pieces and mechanically milled into 20-mesh powders. The food-additive-grade KGM with a molecular mass of 1000 kDa that was used in this study was purchased from Hubei Konson Konjac Gum Co., Ltd., China. All chemicals were of high purity and were purchased from Fluka, Aldrich or Merck. Analytical reactions were carried out in 1 mL or 5 mL V-vials in a heating block with an evaporating unit that was obtained from Barkey GmbH & Co. KG, Germany.

2.2. Extraction of SGM

The method used for SGM extraction was based on the method developed by Zhang, Li, Lindstroem, Stepan, and Gatenholm (2013). Wood powders were mixed with acetone and allowed to stand overnight to remove the extractives. After the acetone was filtered off, the wood powders were delignified using HOAc and $NaClO_2$ for 7 h to obtain holocellulose. The holocellulose was then added to a $NaOH/H_3BO_3$ (17.5/4.0%) solution in a polyethylene bottle and shaken overnight under an N_2 atmosphere. The solution was filtered out, and Fehling solution was added to the solution until no further precipitation of the copper complex was observed. The precipitates were then dissolved in HCl, washed and subsequently re-precipitated using 70%, 96% and, finally, pure ethanol, followed by freeze drying. To purify the SGM, the materials were dissolved in water and dialyzed (molecular weight cut off (MWCO): 3.5 kDa). The yield of isolated SGM was 6.7% with respect to the starting wood powders. The average molecular weight (M_w) of the SGM was determined to be 10 kDa using alkaline size-exclusion chromatography (SEC).

2.3. Carbohydrate and linkage analysis of SGM and KGM

The carbohydrate compositions of the SGM and KGM were determined following the standard procedures for the Tappi test method T222 om-06 (2006) using a High-Performance Anion-Exchange Chromatograph (HPAEC-PAD, Dionex, Sunnyvale, CA, USA) for mono-sugar quantification directly following the acid hydrolysis.

The glycosyl linkage analysis was performed at the Complex Carbohydrate Research Center (The University of Georgia) according to the method described by York, Darvill, McNeil, Stevenson, and Albersheim (1986). The samples were permethylated, depolymerized, reduced and acetylated, and the resultant partially methylated alditol acetates (PMAAs) were analyzed *via* gas chromatography–mass spectrometry (GC–MS).

2.4. Preparation of partially methylated glucomannans with different DS values

The KGM and SGM were well dissolved in H_2O and DMSO, respectively. The methylation of the KGM was performed in H_2O with NaOH/MeI, while the SGM was methylated in DMSO with Li-dimsyl/MeI, both at room temperature. The reactions were carried out under nitrogen. The partially methylated samples were isolated *via* dialysis (MWCO: 3.5 kDa) and freeze dried. Partially methylated spruce glucomannan (MeSGM) and partially methylated konjac glucomannan MeKGM were obtained. The definition of the DS is the average number of substituted OH groups per anhydroglucose unit (Kato, Kawaguchi, & Mizuno, 1973), which can take values between 0 and 3. The base 1.6 M Li dimsyl ($CH_3SOCH_2^-$ Li^+) was freshly prepared, and NaOH was freshly finely pulverized. The methylation conditions are summarized in Table 1. The molar compositions of the various MeSGM and MeKGM samples were determined *via* GLC after hydrolysis, reduction and acetylation according to the method followed in previous studies (Adden, Niedner, Mueller, & Mischnick, 2006; Voiges, Adden, Rinken, & Mischnick, 2012). The DS values were obtained *via* gas chromatography. MeSGM1, MeSGM2 and MeKGM1, along with the SGM and KGM, were used to study the effects of methylation modification on the thermal degradation behavior and kinetics.

For the quantitative measurement of alditol acetates obtained from partially methylated GMs *via* gas liquid chromatography

Table 1
Methylation conditions and degree of substitution of spruce and konjac glucomannans.

Sample name	Reagent (base and solvent)	Base [equiv/unit]	Concentration [mg/mL]	CH_3I [equiv/unit]	Reaction time [h]	Total DS	χ_2		χ_3		χ_6	
							Man	Glc	Man	Glc	Man	Glc
MeSGM1	Li-dimsyl/DMSO	0.8	10	1.2	2	0.71	0.22	0.39	0.31	0.38	0.12	0.16
MeSGM2	Li-dimsyl/DMSO	2	10	3	3	2.04	0.77	0.88	0.77	0.76	0.48	0.45
MeKGM1	NaOH/H_2O	4	25	4	24	1.06	0.44	0.53	0.30	0.15	0.33	0.35

The incubation time with the base for all reactions was 15 min. Each DS value is the average of duplicate determinations.
χ_i is the partial DS value at position i (i refers to positions 2, 3 and 6).

(GLC) using a flame ionization detector (FID), the effective carbon response (ECR) concept was applied (Sweet, Shapiro, & Albersheim, 1975).

2.5. Thermogravimetric measurements

Dynamic thermogravimetric analysis was performed using a Mettler-Toledo 851 (TGA/SDTA) module (Mettler Toledo, Columbus, OH). A nitrogen atmosphere (50 ml/min) and various heating rates in the range of 3–20 °C/min in the temperature range between 25 °C and 750 °C were used to assess the thermal degradation behavior and kinetics. The data for the resulting experimental curves were closely spaced and contained more than 2000 points. On the other hand, both nitrogen and oxygen atmospheres were used in the same method, following García et al. (2013), to perform a proximate analysis of the studied materials. This thermogravimetric method consisted of a heating ramp of 50 °C/min from 25 °C to an isothermal 120 °C for 3 min, followed by a new 100 °C heating ramp programmed to 950 °C, and, finally, a cooling process of −100 °C/min to 450 °C. The proximate analysis data (ash, volatile matter and fixed carbon) were obtained by the direct measure of the weight changes in each experimental curve. The obtained percentages for the ash [Ash], volatile matter [VM] and fixed carbon [FC] contents of each glucomannan were used to assess the net heating value (NHV). The NHV of each sample was calculated using the best equation among the 13 studied correlations proposed by Erol, Haykiri-Acma, and Küçükbayrak (2010). This equation (Eq. (1)) exhibited the highest accuracy for the estimation of the NHVs of biomass samples and their statistical performance criteria.

$$\begin{aligned}\mathrm{NHV} = {} & -116 - 1,33[\mathrm{Ash}] - 0,005[\mathrm{VM}] + 1,92[\mathrm{VM} + \mathrm{Ash}] \\ & - 0,0227[\mathrm{VM}\cdot\mathrm{Ash}] - 0,0122[\mathrm{VM}]^2 + 0,0299[\mathrm{Ash}]^2 \\ & + 6133[\mathrm{OM}]^{-1} - 0,82[\mathrm{Ash}]^{-1} \end{aligned} \quad (1)$$

The organic matter [OM] was calculated from the difference between the volatile material and the ash content.

2.6. Thermal degradation kinetics

Thermal degradation kinetics should be assessed by determining the three parameters (Ea, $f(\alpha)$ and A) included in the kinetic triplet (Núñez, Fraga, Núñez, & Villanueva, 2000; Sun, Huang, Gong, & Cao, 2006). These parameters can be experimentally determined in two ways: isothermally, with temperature maintained constant over time, or non-isothermally, with the variation in both temperature and time dependent on the heating rate (β). Some methods are based on a single-β model fitting, whereas others are multiple-heating-rate model-free methods, also known as isoconversional methods. The isoconversional methods are considered to be the best approach for truly determining the apparent Ea.

In this work, two different isoconversional methods, the differential Friedman method (Friedman, 1964) and the integral Flynn-Wall-Ozawa method (Ozawa, 1965), were first used to determine the apparent Ea. The obtained values from the different methods were compared to verify their reliability. All kinetic studies assume that the rate of the chemical reaction, $d\alpha/dt$, can be expressed as a function of two quantities: the degree of conversion, $\alpha = (w_0 - w)/(w_0 - w_\infty)$, where w, w_0 and w_∞ are the actual, initial and final weights of the sample, respectively, and the kinetic constant $k(T) = A\exp(-Ea/RT)$, where T is the absolute temperature and R is the gas constant (Eq. (2)). Thermogravimetric-analysis experiments can be performed at a constant rate of heating, $\beta = dT/dt$; therefore, Eq. (2) leads to Eq. (3).

$$\frac{d\alpha}{dt} = f(\alpha)\cdot k(T) \quad (2)$$

$$\frac{d\alpha}{dT} = \frac{A}{\beta}\cdot\exp\left(\frac{-Ea}{RT}\right) f(\alpha) \quad (3)$$

By taking the logarithms of both sides of Eq. (3), the first proposed differential Friedman method (Eq. (4)) is obtained.

$$\ln\left(\frac{d\alpha}{dt}\right) = \ln Af(\alpha) - \frac{Ea}{RT} \quad (4)$$

By taking the integrals of both sides of Eq. (3) and assuming α_0 and T_0 to be equal to zero, Eqs. (5) and (6), respectively, are obtained.

$$\int_{\alpha_0}^{\alpha_p}\frac{d\alpha}{f(\alpha)} = \frac{A}{\beta}\int_{T_0}^{T_p}\exp\left(\frac{-Ea}{RT}\right)\,dT \quad (5)$$

$$g(\alpha) = \int_0^{\alpha_p}\frac{d\alpha}{f(\alpha)} = \frac{A}{\beta}\int_0^{T_p}\exp\left(\frac{-Ea}{RT}\right)\,dT \quad (6)$$

where $g(\alpha)$ is the integral function of conversion.

By taking logarithms and using the Doyle approximation (Doyle, 1965), Eq. (6) can be rewritten as Eq. (7); this equation is known as the Flynn-Wall-Ozawa method.

$$\log\ \beta = \log\frac{AEa}{g(\alpha)R} - 2.315 - 0.4567\left(\frac{Ea}{RT}\right) \quad (7)$$

The apparent Ea values that were obtained using the isoconversional methods were used as a reference to determine the most suitable kinetic model $f(\alpha)$. The Coats–Redfern method was used to calculate the apparent Ea values from the proposed $f(\alpha)$ forms (Table 2).

In the Coats–Redfern model (Coats & Redfern, 1964), the asymptotic approximation $(2RT/Ea)\to 0$ is applied to solve Eq. (6), and by taking natural logarithms, the model can be rewritten in the following form, Eq. (8):

$$\ln\frac{g(\alpha)}{T^2} = \ln\ \frac{AR}{\beta Ea} - \frac{Ea}{RT} \quad (8)$$

The Coats–Redfern Ea values were compared to the previously obtained isoconversional Ea values to select the most suitable $f(\alpha)$ and, later, to determine the pre-exponential factor A.

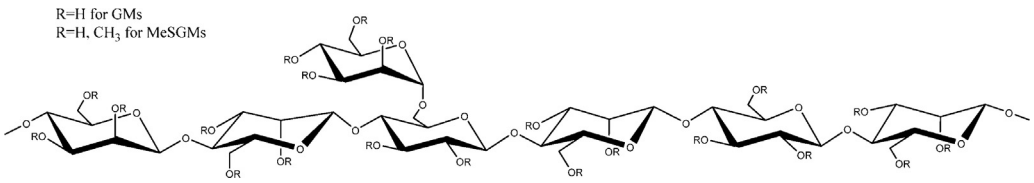

Fig. 1. Proposed structures for spruce glucomannan and its partially methylated derivatives.

3. Results and discussion

3.1. Structure of glucomannans

Both investigated glucomannans, SGM and KGM, are β-1,4-linked glycans (Fig. 1). The average molecular weight of KGM is 1000 kDa, and that of SGM is 10 kDa. According to the carbohydrate analysis, the mannose:glucose ratio was 3.75 for SGM and 1.46 for KGM. The results of the linkage analysis indicated that, compared with the KGM, the SGM had much more terminal mannopyranosyl residue (10.5%) because of its lower molecular weight and branching units (6.8%, mostly 4,6-linked mannopyranosyl residues and 4,6-linked glucopyranosyl residue (4,6-Glc)). In contrast, the KGM contained only 0.7% terminal mannopyranosyl residues and 0.4% branches (2,4-linked glucopyranosyl residue, 2,4-linked galactopyranosyl residue and 4,6-linked mannopyranosyl residue).

As reported by Albrecht et al. (2011), little is known about the precise structure of KGM, especially the sequence of glucose and mannose within the backbone. Blockwise and random distributions have been proposed by the carbohydrate researchers Shimahara, Suzuki, Sugiyama, and Nisizawa (1975) and Cescutti, Campa, Delben, and Rizzo (2002). The DS of each partially methylated glucomannan was obtained, and these data are summarized in Table 1. By applying different equivalents of base per sugar unit and alkylating reagents, different DS values of 0.71 (MeSGM1) and 2.04 (MeSGM2) for SGM and 1.06 (MeKGM1) for KGM were obtained.

3.2. Thermal degradation and pyrolysis characteristics

The thermal degradation of the glucomannan polymers was analyzed in detail *via* dynamical TGA at different heating rates (β). Fig. 2a and b displays the thermogravimetric (TG) and derivative thermogravimetric (DTG) curves of SGM and KGM at various β. Similar profiles were obtained for each material, with a small displacement toward higher temperatures with increasing β, which indicates that the pyrolysis is a thermodynamic process and that a higher β leads to a higher decomposition temperature. However, all these thermograms display several weight-loss stages, allowing a "zonification scheme" (Table 3), in which the volatiles released during the pyrolysis were classified and no significant changes were observed due to the variation of β.

Zone I, which represents more than 10% of the total weight loss for the SGM and 5% for the KGM, lies between 25 °C and 150 °C and is related to the loss of moisture. Zone II (from 200 °C to 375 °C) displays a complex thermal decomposition region with two main overlapping peaks, in which devolatilizations of more than 66% and 59% are observed for SGM and KGM, respectively. From the DTG curves of the KGM, the two main peaks can be clearly identified to have temperatures centered between 266 °C and 292 °C and between 287 °C and 313 °C, depending on β. However, for the SGM, the first peak (between 265 °C and 280 °C) completely overlaps with the second (between 287 °C and 312 °C). The identification of these peaks is complex, and to clarify the different chemical reactions occurring in these overlapping thermal degradation processes, various literature was taken into account. Shen et al. (2010) studied the pyrolytic behavior of the hemicellulose xylan and also identified two peaks in this region: the first peak was assigned to the cleavage of the glycosidic bonds and the decomposition of the side-chain structure, and the second was assigned to the fragmentation of the depolymerized xylan units. Similar to xylan, the first peak of the glucommanan might be related to the cleavage of the glycosidic bonds, and the second might be related to the monomer decomposition itself. However, in this temperature range, it is known that mannose and glucose both decompose in two stages (Hajaligol, Waymack, & Kellogg, 1999; Räisänen, Pitkänen, Halttunen, & Hurtta, 2003). Räisänen et al. identified two peaks for the decomposition of mannose: the first one had an onset temperature of 207 °C and a weight loss of 70%, and the second had an onset temperature of 308 °C and a residual weight loss of 30%. Moreover, in this region, glucose undergoes major decomposition, with two main peaks at 230 and 270–312 °C representing approximately 26% and 74% of the total material, respectively. Based on this information, the first overlapped peak found in Zone II could be related to the greater part of the mannose units, and the higher one could be associated with the degradation of the greater part of the glucose units. Furthermore, C. Ramos-Sanchez et al. (1988) studied the thermal differences between the α- and β-linked stereoisomers, concluding that β-1,4 linkages present higher thermal stability than α-1,4 linkages. This is plausible because the cleavage of the glycosidic linkages of hexaparanosides starts with an intramolecular attack on the primary OH of C-6 at the anomeric carbon to form 1,6-anhydrosugars. For α-linked glycans, this attack is stereochemically favored. The monosaccharide units have similar structures, but the hydroxyl groups at C-2 and C-3 in mannose have a *cis* configuration, while they have a *trans* configuration in glucose. Consequently, the D-glucosyl residues are thermally more stable than the D-mannosyl residues. Zone III appears as a tail at higher temperatures (>375 °C), which is primarily related to the pyrolysis of a portion of the previously formed char. Both glucomannans display a weight loss of approximately 9% in this final zone.

A deeper insight into the assignment of the peaks in Zone II (related to the most intense devolatilization region) was essayed

Table 2
Algebraic expressions of functions representing the most common reaction mechanisms involved in solid-phase reactions.

Kinetic models	Differential form $f(\alpha)$	Integral form $g(\alpha)$
Diffusion models		
1-D diffusion (D1)	$\frac{1}{2}(1-\alpha)-1$	α^2
2-D diffusion (D2)	$-\ln(1-\alpha)$	$((1-\alpha)\ln(1-\alpha))+\alpha$
3-D diffusion-Jander (D3)	$3/2(1-\alpha)^{2/3}(1-(1-\alpha)^{1/3})^{-1}$	$((1-(1-\alpha)^{1/3})^2$
Geometrical contraction models		
Contracting area (R2)	$2(1-\alpha)^{1/2}$	$1-(1-\alpha)^{1/2}$
Contracting volume (R3)	$3(1-\alpha)^{2/3}$	$1-(1-\alpha)^{1/3}$
Reaction-order models		
Zero order (F0/R1)	1	α
1st order (F1)	$(1-\alpha)^1$	$-\ln(1-\alpha)$
nth order (Fn for $n>1$)	$(1-\alpha)^n$	$1-(1-\alpha)/(1-n)$
Nucleation models		
Avrami-Erofeyev (A2)	$2(1-\alpha)(-\ln(1-\alpha))^{1/2}$	$-(\ln(1-\alpha))^{1/2}$
Avrami-Erofeyev (A4)	$4(1-\alpha)(-\ln(1-\alpha))^{3/4}$	$-(\ln(1-\alpha))^{1/4}$
Power law (P2)	$2\,\alpha^{1/2}$	$\alpha^{1/2}$

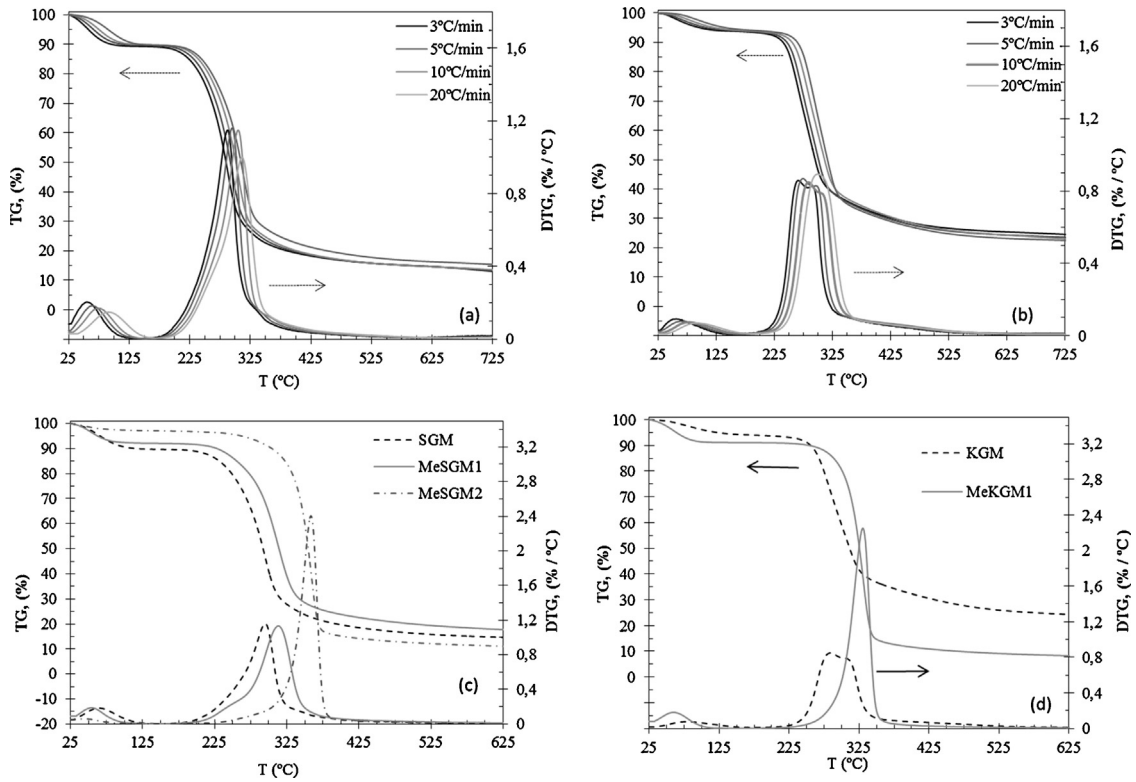

Fig. 2. TG and DTG curves for (a) SGM and (b) KGM; (c) comparison of SGM and its methylated derivatives MeSGM1 (DS 0.68) and MeSGM2 (DS 2.14) at 10 °C/min, and (d) comparison of KGM and its methylated derivative MeKGM 1 (DS 1.06) at 10 °C/min.

to verify that the first peak is related to the thermal decomposition of the majority of the mannose and that the second is related to the pyrolysis of the glucose. Fig. 3 displays the DTG curves of both monomers (glucose and mannose) and compares these curves to that obtained for the SGM, verifying our previous statement.

Table 4 correlates the changes in the volatile yield with the changes in the char yields, the changes in the maximum rate of pyrolysis and the changes in the devolatilization temperatures (onset, temperature at maximum rate, termination) for SGM and KGM. The onset is related to the initial decomposition temperature of Zone II, and the termination is related to the involution point.

It is apparent that each glucomannan presents its own typical decomposition characteristics. The SGM exhibits a larger volatile yield and higher reactivity at the maximum decomposition temperature (~83%, 1.15 wt% °C^{-1}) than the KGM (~73%, ~0.8 wt% °C^{-1}). On the other hand, the KGM exhibits higher onset

Table 3
Distribution of volatiles released during glucomannan pyrolysis.

	Heating rate (°C/min)	Moisture (%)	Distribution of volatiles (%)		Total volatiles (%)
		Zone I (<150 °C)	Zone II (200–375 °C)	Zone III (>375 °C)	
SGM	3	10.8 ± 0.2	68.2 ± 0.2	8.8 ± 0.2	87.8 ± 0.2
	5	10.2 ± 0.3	68.0 ± 0.2	8.5 ± 0.4	86.7 ± 0.3
	10	10.4 ± 0.3	67.5 ± 0.4	9.1 ± 0.5	87.0 ± 0.4
	20	10.3 ± 0.2	66.8 ± 0.6	9.5 ± 0.5	86.5 ± 0.5
MeSGM1	3	7.6 ± 0.2	66.1 ± 0.2	9.0 ± 0.2	82.7 ± 0.2
	5	8.1 ± 0.2	65.3 ± 0.2	9.4 ± 0.2	82.8 ± 0.2
	10	7.8 ± 0.2	66.0 ± 0.3	9.6 ± 0.3	83.4 ± 0.3
	20	7.8 ± 0.2	64.9 ± 0.4	9.7 ± 0.3	82.4 ± 0.4
MeSGM2	3	1.9 ± 0.2	85.9 ± 0.3	2.7 ± 0.3	90.5 ± 0.3
	5	3.0 ± 0.3	84.5 ± 0.5	2.4 ± 0.5	89.9 ± 0.5
	10	2.9 ± 0.2	85.2 ± 0.5	2.0 ± 0.2	90.1 ± 0.4
	20	2.2 ± 0.2	85.8 ± 0.3	1.6 ± 0.3	89.6 ± 0.3
KGM	3	6.1 ± 0.2	59.6 ± 0.3	9.3 ± 0.1	75.0 ± 0.3
	5	5.9 ± 0.2	60.2 ± 0.4	9.8 ± 0.2	76.0 ± 0.3
	10	5.7 ± 0.2	59.4 ± 0.3	11.6 ± 0.5	76.6 ± 0.4
	20	5.2 ± 0.3	61.4 ± 0.4	10.2 ± 0.4	76.9 ± 0.4
MeKGM1	3	7.9 ± 0.2	83.3 ± 0.2	1.5 ± 0.2	92.9 ± 0.2
	5	8.5 ± 0.2	83.3 ± 0.2	1.2 ± 0.3	93.0 ± 0.3
	10	8.9 ± 0.2	82.4 ± 0.2	1.2 ± 0.2	92.6 ± 0.2
	20	8.7 ± 0.2	81.6 ± 0.4	1.1 ± 0.4	91.5 ± 0.4

Each value is the average of duplicate determinations.

Table 4
TG parameters for the glucomannan samples at various heating rates.

	Heating rate (°C/min)	Yield (wt% db)[a]		Max. rate (%°C^{-1})	Temp at max. rate (°C^{-1})	Onset (°C)	Termination (°C)
		Volatiles	Char[b]				
SGM	3	83.2 ± 0.2	16.7 ± 0.2	1.15	286.8 ± 0.2	218.1 ± 0.9	367.2 ± 0.9
	5	83.5 ± 0.2	16.6 ± 0.2	1.15	293.1 ± 0.3	230.2 ± 1.5	378.8 ± 1.0
	10	83.4 ± 0.2	16.5 ± 0.2	1.15	304.8 ± 0.2	243.4 ± 1.0	389.1 ± 0.8
	20	82.6 ± 0.5	18.5 ± 0.5	1.00	312.1 ± 0.4	254.4 ± 1.5	412.2 ± 1.2
MeSGM 1	3	79.8 ± 0.2	20.1 ± 0.2	1.16	296.3 ± 0.3	229.7 ± 0.8	365.2 ± 0.8
	5	80.1 ± 0.1	19.6 ± 0.1	1.16	303.9 ± 0.1	235.5 ± 0.9	376.0 ± 1.5
	10	79.9 ± 0.1	20.1 ± 0.1	1.17	314.2 ± 0.2	248.3 ± 1.1	393.5 ± 1.5
	20	79.3 ± 0.3	20.7 ± 0.3	1.15	324.2 ± 0.2	261.1 ± 1.3	409.2 ± 1.6
MeSGM 2	3	87.5 ± 0.4	11.6 ± 0.4	2.65	340.9 ± 0.2	268.9 ± 1.0	367.9 ± 0.9
	5	87.4 ± 0.5	12.2 ± 0.5	2.57	348.1 ± 0.2	282.1 ± 1.2	380.2 ± 0.8
	10	88.4 ± 0.1	11.6 ± 0.1	2.40	359.2 ± 0.2	294.5 ± 1.1	391.1 ± 0.9
	20	88.1 ± 0.3	11.6 ± 0.3	1.97	369.9 ± 0.3	334.3 ± 1.5	417.2 ± 1.8
KGM	3	73.1 ± 0.6	26.9 ± 0.6	0.85	266.0 ± 0.2	244.4 ± 1.0	370.1 ± 0.8
	5	73.8 ± 0.3	26.1 ± 0.1	0.85	274.3 ± 0.3	252.1 ± 0.9	381.0 ± 0.9
	10	73.9 ± 0.2	26.2 ± 0.2	0.83	282.1 ± 0.5	263.2 ± 0.9	390.7 ± 0.8
	20	74.2 ± 0.1	24.7 ± 0.1	0.88	292.5 ± 1.6	285.4 ± 1.2	413.8 ± 1.2
MeKGM 1	3	90.9 ± 0.1	9.1 ± 0.1	2.18	310.2 ± 0.2	262.9 ± 1.2	353.0 ± 0.9
	5	90.4 ± 0.2	9.6 ± 0.2	2.35	321.3 ± 0.4	277.0 ± 1.5	365.4 ± 1.0
	10	90.8 ± 0.1	9.2 ± 0.1	2.22	331.3 ± 0.4	287.2 ± 1.6	371.2 ± 1.3
	20	89.9 ± 0.4	10.1 ± 0.4	1.99	338.5 ± 0.6	299.2 ± 1.5	355.9 ± 1.0

Each value is the average of duplicate determinations. The deviations of the maximum rate are <0.1.
[a] db, dry base content.
[b] Comprises the fixed carbon at 600 °C and the ash content.

values (245–285 °C *vs.* 218–254 °C), higher char yields (~27% *vs.* 17%) and more rapid thermal decomposition (ΔT = 124 °C *vs.* 150 °C). The differences in the volatile distributions could be related to the mannose:glucose ratio of the starting materials. From this perspective, a higher mannose content seems to represent larger amounts of volatiles. In addition, the higher thermal stability of the KGM could be attributable to its higher molecular weight, but chemical composition and structure also play a significant role in this phenomenon. C. Ramos-Sanchez et al. (1988) studied the relationships between molecular structure and thermal behavior, determining that when depolymerization occurs *via* glycosidic bond cleavages, differences are observed in the thermal behavior of disaccharides and polymer carbohydrates, with the glycoside linkages between the glucose being the most resistant. This fact suggests that the sequence of glucose and mannose units within the backbone could also influence the thermal stability of glucomannan polymers.

The thermal degradation of the methylated glucomannans was also investigated, and the results were compared with those of the corresponding non-modified glucomannans (Fig. 2c and d). The profiles of the SGM and KGM TG curves changed because of the methylation, resulting in a more homogeneous material with a narrower thermal-decomposition region. Table 3 summarizes the distribution of the volatiles released during the pyrolysis of the methylated glucomannan. In the case of the methylated SGM, a decrease was observed in the volatile content of Zone I (from 10% to 3%), an increase was observed in the yield of Zone II (from 66% to 85%), and a decrease was observed in Zone III (from 9% to 2%) as the DS increased (Table 3). Similar trends were observed for the methylated KGM, leading to similar product distributions for MeSGM2 and MeKGM1. The thermogravimetric parameters of the modified glucomannans are also displayed in Table 4. A decrease in the char content and increases in the maximum rate, temperature peak, and onset were observed as the DS increased. In addition, because 6-OH is involved in the decomposition, the degree of branching at O-6 in the SGM, in addition to the degree of methylation at O-6 (the partial DS value at position 6 increased from 0.16 to 0.45), stabilized the SGM. The lower char values for the modified sample are related to the replacement of the water loss observed for the SGM and KGM with the loss of methanol for the methylated samples, as the molecular weight of methanol is higher than that of water.

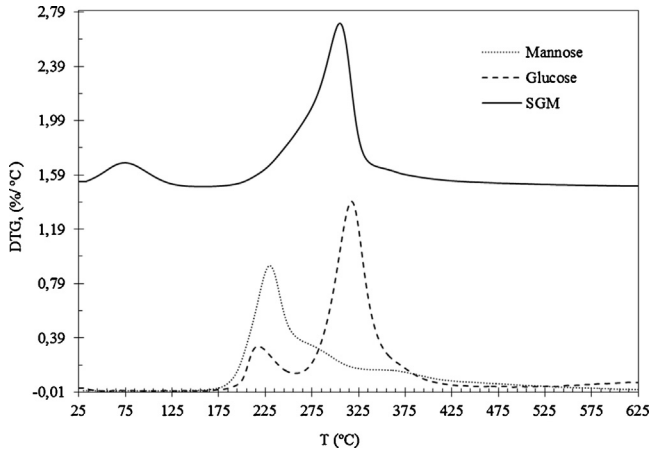

Fig. 3. Comparative DTG curves for the assignment of the SGM peaks.

MeSGM2, with a DS of 2.04, exhibited the maximum thermal stability, with an increase of more than 50 °C with respect to the SGM; it was found to be the most thermally resistant polymer among all studied. At this DS, 45% of the primary OHs at position 6 are blocked, and thus the initial cleavage of the glycosidic linkages is prohibited. MeSGM2 appears to possess onset values (333 °C) that are comparable to those of other commercial thermoplastic carbohydrates, such as polylactic acid and thermoplastic starch (Badía, Santonja-Blasco, Moriana, & Ribes-Greus, 2010; Moriana, Karlsson, & Ribes-Greus, 2010). The relatively higher onset values of MeSGM2 demonstrate this polymer to be the most attractive for subjection to high-temperature processing operations and for application as a more thermally stable biomaterial, such as for use as a polymer matrix in composites. At the same time, the lower increase in temperature necessary to reach total conversion

($\Delta T = 80\,^{\circ}C$), the higher volatile content (88%) and the higher reactivity ($0.8\ wt\%\,^{\circ}C^{-1}$) of this modified polymer make it interesting for use in the production of gas resources.

However, when considering biomass thermal-conversion technologies, proximate analysis is one of the most important characterization methods to consider because of the neat heating value, which determines the energy value of the assessed material (García et al., 2013). Table 5 shows the proximate analysis using both inert and oxidative atmospheres and the calorific values (NHVs) calculated according to Eq. (1).

The net calorific values of the glucomannan samples (17.8 and 18.0 MJ/kg for the SGM and KGM, respectively) are consistent with the heating values of hemicellulose previously published by White (1987). The results for the glucomannans and their derivatives are also in agreement with the NHV values that have been reported for other biomass materials, which are in the range of 15.4–19.5 MJ/kg (Erol et al., 2010). These values indicate that glucomannan polymers produce similar heating energies during combustion processes as do lignocellulosic biomass materials.

3.3. Thermal degradation kinetics

Fig. 4a and b shows the conversion-degree rate (α) as a function of temperature for SGM and KGM at various heating rates (β). The differential and integral isoconversional methods of Friedman and Flynn-Wall-Ozawa were first used to determine the apparent *Ea* of all the studied glucomannan polymers. These methods allow the acquisition of the apparent *Ea* from the slope of the isoconversional plots, wherein the derivative of α and $\ln(\beta)$ are represented as functions of temperature. The plots of the isoconversional methods for the SGM and KGM exhibited a general trend of *Ea* values of $0.3 < \alpha < 0.75$, where the fitted lines were parallel. As an example, the Friedman and Flynn-Wall-Ozawa plots for the SGM are shown in Fig. 4c and d, where changes in the parallelism of the fitted lines can be observed at lower ($0.12 < \alpha < 0.3$) and higher ($\alpha > 0.75$) α values.

The apparent *Ea* values as a function of α that were obtained using the Friedman and Flynn-Wall-Ozawa methods are shown in Fig. 5. It can be observed that the values obtained using both isoconversional methods were nearly identical. The dependence of the apparent *Ea* on α can be separated cleanly into three distinct regions for the SGM and KGM: the first region, where small variations in *Ea* are observed, is for values of $0.12 < \alpha < 0.35$; the second region, where *Ea* can be considered to be stable, corresponds to $0.35 < \alpha < 0.75$; and the third region, where a rapid increase in *Ea* is evident, is defined by $\alpha > 0.75$. The first and second α regions correspond to Zone II, where the most intense devolatilization takes place. Therefore, these regions, where $0.12 < \alpha < 0.75$, were selected to be studied in detail.

Table 6 summarizes the average *Ea* values calculated from both conversion ranges: the first region ($0.12 < \alpha < 0.35$), which is related to the first overlapped peak, and the second one ($0.35 < \alpha < 0.75$), where most of the glucose degradation is believed to take place. These changes in *Ea* as a function of α indicate that a complex mechanism exists for the thermal degradation of the glucomannans.

For lower α ($0.12 < \alpha < 0.35$), it was possible to calculate apparent *Ea* values of 226–230 kJ/mol and 180–185 kJ/mol for SGM and KGM, respectively. For higher α ($0.35 < \alpha < 0.75$), the values were found to be 218–219 and 206 kJ/mol for SGM and KGM, respectively. In general, the apparent *Ea* values of the SGM are higher than those obtained for the KGM. Specifically, at lower α, the *Ea* of SGM is 40 kJ/mol higher than that of KGM, indicating that the slower degradation rate may be attributable to the higher mannose content and to the branching units present in the SGM. These calculated *Ea* values are much higher than that reported by Branca et al. (2013) of approximately 96 kJ/mol. These differences could be attributable to the fact that these authors assumed a mechanism consisting of two competing first-order reactions to calculate the *Ea* values. As mentioned above, the Friedman and Flynn-Wall-Ozawa methods permit the determination of the apparent *Ea* without precise knowledge of the reaction mechanisms, so it is believed that using these iso-conversional methods is a more accurate way to obtain the *Ea* values. In comparison with other thermal degradation kinetics studies for carbohydrates, Akbar et al. (2012) reported *Ea* values for pentose- and hexose-based carbohydrate polymers that were closer to our estimated *Ea* (approximately 157–167 kJ/mol), while Miller & Bellan (1997) also reported higher values for hemicellulose reactions (202 kJ/mol) and Iqbal et al. (2013) determined average *Ea* values in the range of 132–187 kJ/mol for 9 different polysaccharide materials.

The trend in the apparent *Ea* as a function of α for the methylated samples was also evaluated. The apparent *Ea* values are nearly constant in the $0.2 < \alpha < 0.8$ range, which implies the possibility of a single reaction mechanism or the unification of multiple reaction mechanisms. The first conversion region is shorter than in the non-methylated glucomannans, resulting in a more homogenous material, as stated before. For both glucomannans, a decrease in *Ea* with increasing DS was observed, indicating an enhancement in the degradation rate caused by methylation.

The *Ea* values that were obtained using the Friedman and Flynn-Wall-Ozawa methods were used as a reference to assess the most probable kinetic model for each thermal decomposition process. In solid-state reactions, a model is a rate equation that can describe a type of reaction (Khawam & Flanagan, 2006). Many solid-state kinetic models have been developed in the past century and are classified according to their mechanistic basis as nucleation, geometrical contraction, diffusion, and reaction-order models. The Coats–Redfern method was used to calculate the *Ea* values from the various proposed kinetics models, the algebraic expressions for which are shown in Table 2. Table 7 summarizes the different apparent *Ea* values for each conversion range, where *Ea*1 and *Ea*2 are the values obtained for the lowest and highest α values in Zone II (most intense devolatilization region), respectively.

The Dn and Fn kinetic models were selected for both glucomannans on the basis of the similarity of their *Ea* values to those determined using the isoconversional methods. Iqbal et al. (2013) demonstrated good fits with both these kinetic models for predicting the pyrolysis of various carbohydrate polymers. In addition, Akbar et al. (2012) demonstrated that certain hexose-based carbohydrate polymers follow D4 mechanisms for the pyrolysis of the major degradation stage.

The pyrolysis of SGM can be modeled using a complex mechanism that involves a D3-type reaction followed by an F3.25-type reaction. Similarly, the pyrolitic behavior of KGM can be described in terms of a D2 diffusional model followed by an F3.25 model. Therefore, the thermal degradation of both glucomannans for $0.35 < \alpha < 0.75$ can be explained using an order-based model, which indicates that the reaction rate is proportional to the remaining fraction of reactants. At lower α, diffusion plays an important role; solid-state reactions often occur between crystal lattices or with molecules that must permeate into lattices where motion is restricted (Khawam & Flanagan, 2006). The D3 model is based on the assumption of spherical solid particles, whereas the D2 model assumes radial diffusion through a cylindrical shell.

Various changes in the kinetic modeling can be observed as a result of the methylation of the glucomannans. While MeSGM1 still follows the D3 and F3.25 models, the D1 model followed by the F1 model is the best description of the degradation of MeSGM2. For the kinetic modeling of the KGM, the reaction type changed from D2 to D1 at lower α and from F3.25 to F1 at higher α. The similar thermal behavior that was observed

Table 5
Glucomannan proximate analysis using thermogravimetry.

Sample	Ash (%)	Volatiles (%)	Fixed carbon (%)	Organic matter (%)	NHV (MJ/kg)
SGM	3.9 ± 0.2	83.6 ± 0.4	12.5 ± 0.3	96.8 ± 0.4	17.8 ± 0.4
MeSGM1	5.0 ± 0.4	81.0 ± 0.6	15.0 ± 0.4	95.0 ± 0.6	18.0 ± 0.6
MeSGM2	3.2 ± 0.2	88.0 ± 0.5	8.8 ± 0.3	96.8 ± 0.5	17.0 ± 0.5
KGM	1.7 ± 0.2	73.0 ± 0.6	25.3 ± 0.4	98.3 ± 0.6	18.0 ± 0.6
MeKGM1	2.0 ± 0.3	91.0 ± 0.7	7.0 ± 0.2	98.0 ± 0.7	16.6 ± 0.7

Each value is the average of duplicate determinations.

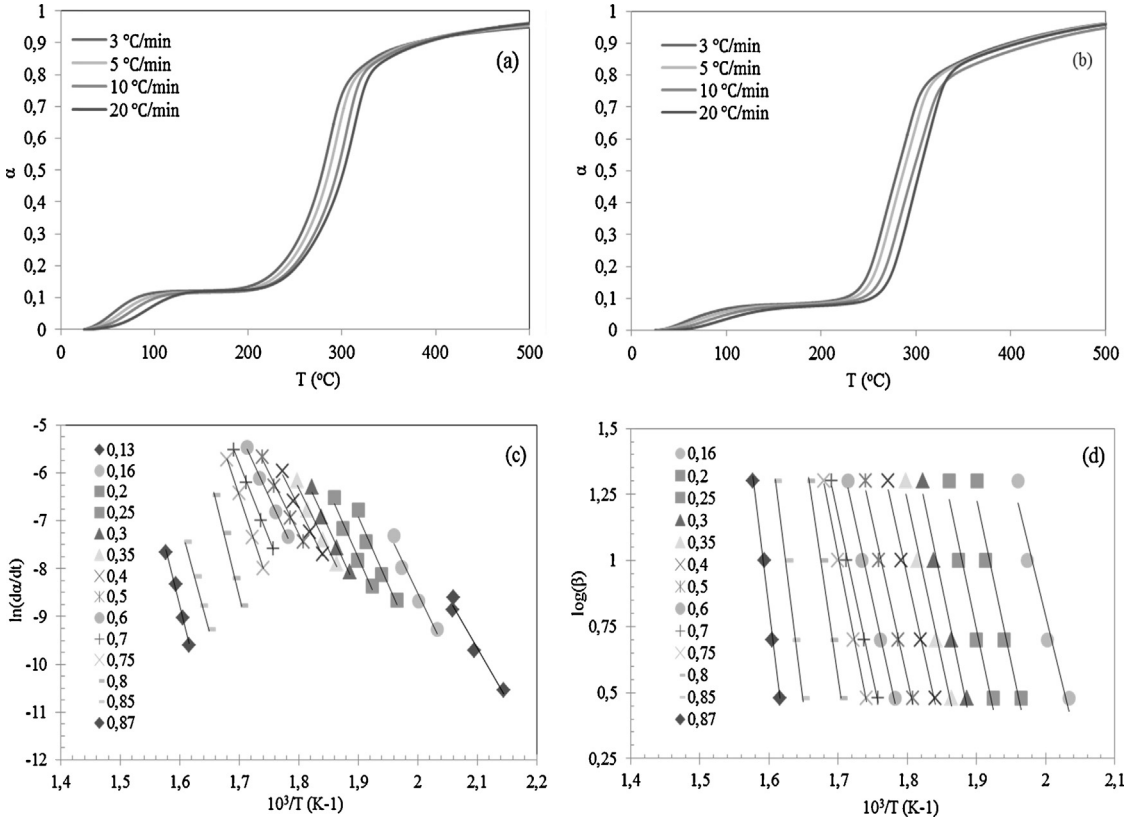

Fig. 4. Degree of conversion as a function of temperature for (a) SGM and (b) KGM at various heating rates. Isoconversional (c) Friedman and (d) Flynn-Wall-Ozawa plots for SGM.

previously between MeSGM2 and MeKGM1 now corresponds to the same kinetic modeling. In diffusion-controlled reactions, the rate of product formation decreases proportionally with the increasing thickness of the product barrier layer. In terms of the kinetics of glucomannans in general, it seems that the barrier layers of KGM and SGM are thicker than those of their methylated derivatives. The reason for this difference could be that, during methylation, methyl groups replace the hydroxyl

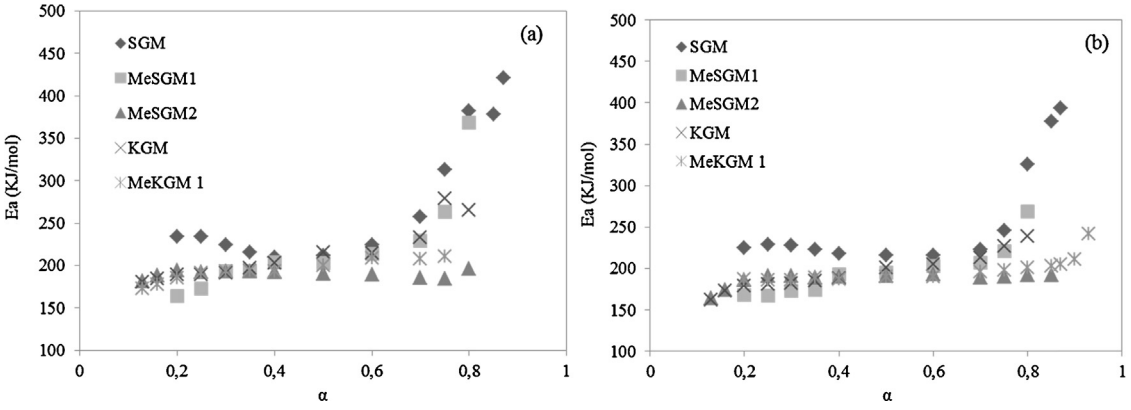

Fig. 5. A comparison of apparent activation energy as a function of degree of conversion (α) for all glucomannan samples using the (a) Friedman and (b) Flynn-Wall-Ozawa methods.

Table 6
Apparent activation energy of glucomannans calculated using the Friedman and Flynn-Wall-Ozawa methods in various degree-of-conversion ranges.

		Friedman		Flynn-Wall-Ozawa	
		Ea (kJ/mol)	R^2	*Ea* (kJ/mol)	R^2
SGM	$0.12 < \alpha < 0.35$	230 ± 6	0.9849 ± 0.0052	226 ± 3	0.9730 ± 0.0154
	$0.35 < \alpha < 0.75$	218 ± 7	0.9960 ± 0.0029	219 ± 4	0.9934 ± 0.0039
MeSGM1	$0.12 < \alpha < 0.25$	169 ± 5	0.9950 ± 0.0048	170 ± 7	0.9995 ± 0.0003
	$0.25 < \alpha < 0.75$	203 ± 9	0.9988 ± 0.0004	200 ± 3	0.9991 ± 0.0011
MeSGM2	$0.12 < \alpha < 0.2$	165 ± 5	0.9890 ± 0.0102	165 ± 3	0.9519 ± 0.0331
	$0.2 < \alpha < 0.8$	191 ± 2	0.9917 ± 0.0053	191 ± 4	0.9912 ± 0.0021
KGM	$0.12 < \alpha < 0.35$	185 ± 6	0.9975 ± 0.0016	181 ± 7	0.9996 ± 0.0003
	$0.35 < \alpha < 0.75$	206 ± 9	0.9716 ± 0.0256	206 ± 6	0.9985 ± 0.0009
MeKGM1	$0.12 < \alpha < 0.2$	175 ± 2	0.9742 ± 0.0070	175 ± 2	0.9700 ± 0.0101
	$0.2 < \alpha < 0.8$	197 ± 9	0.9937 ± 0.0051	194 ± 8	0.9896 ± 0.0052

Each value is the average of duplicate determinations.

Table 7
Ea values for glucomannans determined using the Coats–Redfern equation.

Kinetic models	SGM		MeSGM1		MeSGM2		KGM		MekGM1	
	*Ea*1[a]	*Ea*2[b]	*Ea*1[c]	*Ea*2[d]	*Ea*1[c]	*Ea*2[b]	*Ea*1[a]	*Ea*2[b]	*Ea*1[c]	*Ea*2[d]
1-D diffusion (D1)	203 ± 2	102 ± 2	93 ± 2	127 ± 1	163 ± 3	274 ± 2	170 ± 2	99 ± 1	176 ± 4	218 ± 3
2-D diffusion (D2)	218 ± 4	123 ± 2	98 ± 2	145 ± 3	190 ± 2	314 ± 3	182 ± 2	118 ± 2	199 ± 3	250 ± 4
3-D diffusion-Jander (D3)	226 ± 4	150 ± 1	165 ± 4	169 ± 3	196 ± 2	370 ± 3	197 ± 2	143 ± 2	103 ± 2	290 ± 3
Zero order (F0/R1)	37 ± 3	46 ± 1	42 ± 1	58 ± 2	86 ± 2	131 ± 2	80 ± 1	45 ± 1	43 ± 1	104 ± 2
Contracting area (R2)	41 ± 2	64 ± 1	46 ± 1	74 ± 2	91 ± 2	164 ± 2	90 ± 1	60 ± 1	47 ± 1	148 ± 2
Contracting volume (R3)	42 ± 1	70 ± 1	47 ± 1	80 ± 1	93 ± 1	177 ± 2	94 ± 1	66 ± 1	47 ± 1	140 ± 2
1st order (F1)	41 ± 1	85 ± 1	50 ± 1	90 ± 1	96 ± 2	190 ± 2	80 ± 1	101 ± 2	49 ± 1	192 ± 4
2nd order (F2)	56 ± 1	139 ± 2	60 ± 1	132 ± 2	107 ± 2	301 ± 3	126 ± 2	127 ± 2	54 ± 1	240 ± 3
3rd order (F3)	68 ± 1	206 ± 2	71 ± 1	182 ± 3	112 ± 2	400 ± 3	155 ± 2	187 ± 2	60 ± 1	336 ± 3
3,25th order (F3)	72 ± 1	220 ± 2	73 ± 1	201 ± 2	120 ± 2	454 ± 3	162 ± 2	202 ± 3	62 ± 1	363 ± 3
Avrami-Erofeyev (A2)	37 ± 1	57 ± 1	39 ± 1	61 ± 2	63 ± 1	18 ± 1	65 ± 1	54 ± 1	39 ± 1	96 ± 1
Avrami-Erofeyev (A4)	15 ± 1	14 ± 1	5 ± 1	16 ± 1	25 ± 1	61 ± 1	27 ± 1	12 ± 1	10 ± 1	47 ± 1
Power law (P2)	39 ± 1	48 ± 2	38 ± 1	59 ± 1	95 ± 1	134 ± 2	83 ± 2	46 ± 1	5 ± 1	33 ± 1

Each value is the average of duplicate determinations.
[a] $0.12 < \alpha < 0.35$.
[b] $0.35 < \alpha < 0.75$.
[c] $0.12 < \alpha < 0.2$.
[d] $0.25 < \alpha < 0.8$.

Table 8
Kinetic parameters for glucomannan TGA pyrolysis obtained using the Flynn-Wall-Ozawa, Friedman and Coats–Redfern methods.

		Friedman	Flynn-Wall-Ozawa	Coats–Redfern		
		Ea (kJ/mol)	*Ea* (kJ/mol)	*Ea* (kJ/mol)	$f(\alpha)$	$\ln A\ (s^{-1})$
SGM	$0.12 < \alpha < 0.35$	230 ± 6	226 ± 3	226 ± 4	$3/2(1-\alpha)^{2/3}(1-(1-\alpha)^{1/3})^{-1}$	29 ± 1
	$0.35 < \alpha < 0.75$	218 ± 7	219 ± 4	220 ± 2	$(1-\alpha)^{3,25}$	40 ± 2
MeSGM1	$0.12 < \alpha < 0.25$	169 ± 5	170 ± 7	165 ± 4	$3/2(1-\alpha)^{2/3}(1-(1-\alpha)^{1/3})^{-1}$	21 ± 2
	$0.25 < \alpha < 0.75$	203 ± 9	200 ± 3	201 ± 5	$(1-\alpha)^{3,25}$	38 ± 2
MeSGM2	$0.12 < \alpha < 0.2$	165 ± 5	165 ± 3	163 ± 3	$½(1-\alpha)-1$	17 ± 1
	$0.2 < \alpha < 0.8$	191 ± 2	191 ± 4	190 ± 2	$(1-\alpha)^{1}$	30 ± 2
KGM	$0.12 < \alpha < 0.35$	185 ± 6	181 ± 7	182 ± 2	$-\ln(1-\alpha)$	29 ± 1
	$0.35 < \alpha < 0.75$	206 ± 9	206 ± 6	202 ± 3	$(1-\alpha)^{3,25}$	33 ± 2
MeKGM1	$0.12 < \alpha < 0.2$	175 ± 2	175 ± 2	176 ± 4	$½(1-\alpha)-1$	14 ± 2
	$0.2 < \alpha < 0.8$	197 ± 9	194 ± 8	192 ± 4	$(1-\alpha)^{1}$	22 ± 2

Each value is the average of duplicate determinations.

groups and simultaneously reduce the interactions between the OH groups, leading to a faster rate of degradation for the methylated materials.

To achieve a full kinetic evaluation of the pyrolysis of glucomannans, the pre-exponential factor *A* for each material was determined from the $f(\alpha)$ and the *Ea* values using the Coats–Redfern method. These values are listed in Table 8 along with the other kinetic parameters for all studied glucomannan carbohydrate polymers.

4. Conclusions

The pyrolysis-product distribution, the net heating value and the thermal stability of SGM and KGM were assessed to better understand the thermal behavior of these carbohydrate polymers for use in specific applications. Both glucomannans exhibited high volatile contents (83–73%) and similar calorific values to those of lignocellulosic biomass (16.6–18 MJ/kg); in general, these parameters are considered desirable for the regulation of

gasification processes. The thermal decomposition of both glucomannans occurred in three different zones that corresponded to water release, intense devolatilization and the pyrolysis of char. The intense-devolatilization region, where two overlapping peaks were evident, was evaluated in detail. The thermal stability of the glucomannans was calculated in terms of the onset degradation temperature of this region, and it indicated differences between the SGM and KGM associated with their different chemical compositions and molecular weights. In addition, the thermal degradation kinetics was assessed using the isoconversional Friedman and Flynn-Wall-Ozawa methods along with the Coats–Redfern method. The pyrolysis of both glucomannans can be modeled using a complex mechanism that involves a Dn-type reaction mechanism followed by an Fn-type reaction.

A comparative study with the methylated derivatives of the investigated glucomannans indicated that a higher DS leads to a higher volatiles yield and a more thermally resistant material. These higher thermal-stability values were comparable to those offered by some commercial thermoplastic carbohydrate polymers that are used as matrices in composites. The kinetics and mechanisms of the degradation of the methylated glucomannans indicated an increase in the degradation rate with increasing DS.

From these results, it can be concluded that glucomannan carbohydrate polymers from spruce and konjac root present interesting thermal degradation properties and that partial methylation can be introduced to suit specific applications.

Acknowledgments

The authors would like to acknowledge the Wallenberg and Lars-Erik Thunholms Foundation for the research post-doctoral position granted to Rosana Moriana.

References

Adden, R., Niedner, W., Mueller, R., & Mischnick, P. (2006). Comprehensive analysis of the substituent distribution in the glucosyl units and along the polymer chain of hydroxyethylmethyl celluloses and statistical evaluation. *Analytical Chemistry*, *78*, 1146–1157. http://dx.doi.org/10.1021/ac051484q

Aggarwal, P., Dollimore, D., & Heon, K. (1997). Comparative thermal analysis study of two biopolymers, starch and cellulose. *Journal of Thermal Analysis*, *50*(1–2), 7–17.

Akbar, J., Iqbal, M. S., Massey, S., & Masih, R. (2012). Kinetics and mechanism of thermal degradation of pentose- and hexose-based carbohydrate polymers. *Carbohydrate Polymers*, *90*(3), 1386–1393.

Albrecht, S., van, M. G. C. J., Xu, J., Schols, H. A., Voragen, A. G. J., & Gruppen, H. (2011). Enzymatic production and characterization of konjac glucomannan oligosaccharides. *Journal of Agricultural and Food Chemistry*, *59*, 12658–12666. http://dx.doi.org/10.1021/jf203091h

Badía, J. D., Santonja-Blasco, L., Moriana, R., & Ribes-Greus, A. (2010). Thermal analysis applied to the characterization of degradation in soil of polylactide: II. On the thermal stability and thermal decomposition kinetics. *Polymer Degradation and Stability*, *95*(11), 2192–2199.

Bilbao, R., Millera, A., & Arauzo, J. (1989). Kinetics of weight loss by thermal decomposition of xylan and lignin. Influence of experimental conditions. *Thermochimica Acta*, *143*, 137–148.

Branca, C., Di Blasi, C., Mango, C., & Hrablay, I. (2013). Products and kinetics of glucomannan pyrolysis. *Industrial & Engineering Chemistry Research*, *52*(14), 5030–5039.

Cescutti, P., Campa, C., Delben, F., & Rizzo, R. (2002). Structure of the oligomers obtained by enzymatic hydrolysis of the glucomannan produced by the plant Amorphophallus konjac. *Carbohydrate Research*, *337*(24), 2505–2511.

Chaouch, M., Pétrissans, M., Pétrissans, A., & Gérardin, P. (2010). Use of wood elemental composition to predict heat treatment intensity and decay resistance of different softwood and hardwood species. *Polymer Degradation and Stability*, *95*(12), 2255–2259.

Cheng, L. H., Abd Karim, A., & Seow, C. C. (2008). Characterisation of composite films made of konjac glucomannan (KGM), carboxymethyl cellulose (CMC) and lipid. *Food Chemistry*, *107*(1), 411–418.

Coats, A. W., & Redfern, J. P. (1964). Kinetic parameters from thermogravimetric data. *Nature (London, UK)*, *201*, 68–69. http://dx.doi.org/10.1038/201068a0

Di Blasi, C., & Lanzetta, M. (1997). Intrinsic kinetics of isothermal xylan degradation in inert atmosphere. *Journal of Analytical and Applied Pyrolysis*, *40–41*, 287–303.

Doyle, C. D. (1965). Series approximations to the equation of thermogravimetric data. *Nature (London, UK)*, *207*, 290–291. http://dx.doi.org/10.1038/207290a0

Enomoto-Rogers, Y., Ohmomo, Y., & Iwata, T. (2013). Syntheses and characterization of konjac glucomannan acetate and their thermal and mechanical properties. *Carbohydrate Polymers*, *92*(2), 1827–1834.

Erol, M., Haykiri-Acma, H., & Küçükbayrak, S. (2010). Calorific value estimation of biomass from their proximate analyses data. *Renewable Energy*, *35*(1), 170–173.

Friedman, H. L. (1964). Kinetics of thermal degradation of char-forming plastics from thermogravimetry. Application to a phenolic plastic. *Journal of Polymer Science Part C: Polymer Symposia*, *6*(1), 183–195.

García, R., Pizarro, C., Lavín, A. G., & Bueno, J. L. (2013). Biomass proximate analysis using thermogravimetry. *Bioresource Technology*, *139*, 1–4.

Hajaligol, M., Waymack, B., & Kellogg, D. (1999). Formation of aromatic hydrocarbons from pyrolysis of carbohydrates. *Preprints of Symposia – American Chemical Society, Division of Fuel Chemistry*, *44*, 251–255.

Iqbal, M. S., Massey, S., Akbar, J., Ashraf, C. M., & Masih, R. (2013). Thermal analysis of some natural polysaccharide materials by isoconversional method. *Food Chemistry*, *140*(1–2), 178–182.

Kato, K., Kawaguchi, Y., & Mizuno, T. (1973). Structural analysis of suisen glucomannan. *Carbohydrate Research*, *29*(2), 469–476.

Khawam, A., & Flanagan, D. R. (2006). Solid-state kinetic models: Basics and mathematical fundamentals. *Journal of Physical Chemistry B*, *110*, 17315–17328. http://dx.doi.org/10.1021/jp062746a

Kohyama, K., Kim, K. Y., Shibuya, N., Nishinari, K., & Tsutsumi, A. (1992). Dielectric, viscoelastic and broad-line NMR study of konjac glucomannan films. *Carbohydrate Polymers*, *17*(1), 59–63.

Mikkonen, K., Mathew, A., Pirkkalainen, K., Serimaa, R., Xu, C., Willför, S., et al. (2010). Glucomannan composite films with cellulose nanowhiskers. *Cellulose*, *17*(1), 69–81.

Miller, R. S., & Bellan, J. (1997). A generalized biomass pyrolysis model based on superimposed cellulose, hemicelluloseand liqnin kinetics. *Combustion Science and Technology*, *126*(1–6), 97–137.

Moriana, R., Karlsson, S., & Ribes-Greus, A. (2010). Assessing the influence of cotton fibers on the degradation in soil of a thermoplastic starch-based biopolymer. *Polymer Composites*, *31*(12), 2102–2111.

Moriana, R., Vilaplana, F., Karlsson, S., & Ribes-Greus, A. (2011). Improved thermomechanical properties by the addition of natural fibres in starch-based sustainable biocomposites. *Composites Part A: Applied Science and Manufacturing*, *42*(1), 30–40.

Nelson David, A., Hallen Richard, T., & Theander, O. (1988). . *Formation of aromatic compounds from carbohydrates pyrolysis oils from biomass* (376) American Chemical Society.

Núñez, L., Fraga, F., Núñez, M. R., & Villanueva, M. (2000). Thermogravimetric study of the decomposition process of the system BADGE ($n = 0$)/1,2 DCH. *Polymer*, *41*(12), 4635–4641.

Ozawa, T. (1965). A new method of analyzing thermogravimetric data. *Bulletin of the Chemical Society of Japan*, *38*(11), 1881–1886.

Ramajo-Escalera, B., Espina, A., García, J. R., Sosa-Arnao, J. H., & Nebra, S. A. (2006). Model-free kinetics applied to sugarcane bagasse combustion. *Thermochimica Acta*, *448*(2), 111–116.

C. Ramos-Sanchez, M., Rey, F. J., L. Rodriguez, M., Martin-Gil, F. J., & Martin-Gil, J. (1988). DTG and dta studies on typical sugars. *Thermochimica Acta*, *134*, 55–60.

Raveendran, K., Ganesh, A., & Khilar, K. C. (1995). Influence of mineral matter on biomass pyrolysis characteristics. *Fuel*, *74*(12), 1812–1822.

Räisänen, U., Pitkänen, I., Halttunen, H., & Hurtta, M. (2003). Formation of the main degradation compounds from arabinose, xylose, mannose and arabinitol during pyrolysis. *Journal of Thermal Analysis and Calorimetry*, *72*(2), 481–488.

Seo, D. K., Park, S. S., Hwang, J., & Yu, T.-U. (2010). Study of the pyrolysis of biomass using thermo-gravimetric analysis (TGA) and concentration measurements of the evolved species. *Journal of Analytical and Applied Pyrolysis*, *89*(1), 66–73.

Shen, D. K., Gu, S., & Bridgwater, A. V. (2010). Study on the pyrolytic behaviour of xylan-based hemicellulose using TG–FTIR and Py–GC–FTIR. *Journal of Analytical and Applied Pyrolysis*, *87*(2), 199–206.

Shimahara, H., Suzuki, H., Sugiyama, N., & Nisizawa, K. (1975). Mannan and related compounds. V. Partial purification of β-mannanases from the konjac tubers and their substrate specificity in relation to the structure of konjac glucomannan. *Agricultural and Biological Chemistry*, *39*, 301–312. http://dx.doi.org/10.1271/bbb1961.39.301

Sun, J. T., Huang, Y. D., Gong, G. F., & Cao, H. L. (2006). Thermal degradation kinetics of poly(methylphenylsiloxane) containing methacryloyl groups. *Polymer Degradation and Stability*, *91*(2), 339–346.

Sweet, D. P., Shapiro, R. H., & Albersheim, P. (1975). Quantitative analysis by various g.l.c. response-factor theories for partially methylated and partially ethylated alditol acetates. *Carbohydrate Research*, *40*(2), 217–225.

White, R. (1987). Effect of lignin content and extractives on the higher heating value of wood. *Wood and Fiber Science*, *19*(4), 446–452.

Wilson, L., Yang, W., Blasiak, W., John, G. R., & Mhilu, C. F. (2011). Thermal characterization of tropical biomass feedstocks. *Energy Conversion and Management*, *52*(1), 191–198.

Voiges, K., Adden, R., Rinken, M., & Mischnick, P. (2012). Critical re-investigation of the alditol acetate method for analysis of substituent distribution in methyl cellulose. *Cellulose*, *19*(3), 993–1004.

Xue Jiao He, H. W., Amadou, I., & Qin, X. J. (2012). Textural and rheological properties of hydrolyzed Konjac Glucomannan and Kappa-Carrageenan: Effect of molecular weight, total content, pH and temperature on the mixed system gels. *Emirates Journal of Food and Agriculture*, *24*(3), 200.

Yang, J., Miranda, R., & Roy, C. (2001). Using the DTG curve fitting method to determine the apparent kinetic parameters of thermal decomposition of polymers. *Polymer Degradation and Stability*, *73*(3), 455–461.

Yao, F., Wu, Q., Lei, Y., Guo, W., & Xu, Y. (2008). Thermal decomposition kinetics of natural fibers: Activation energy with dynamic thermogravimetric analysis. *Polymer Degradation and Stability*, *93*(1), 90–98.

York, W. S., Darvill, A. G., McNeil, M., Stevenson, T. T., & Albersheim, P. (1986). Isolation and characterization of plant cell walls and cell wall components. *Methods in Enzymology*, *118*, 3–40.

Zhang, Y., Li, J., Lindstroem, M. E., Stepan, A., & Gatenholm, P. (2013). Spruce glucomannan: Preparation, structural characteristics and basic film forming ability. *Nordic Pulp and Paper Research Journal*, *28*, 323–330.

Zohuriaan, M. J., & Shokrolahi, F. (2004). Thermal studies on natural and modified gums. *Polymer Testing*, *23*(5), 575–579.